

An Experimental Study on Convective Boiling of R-22 and R-410A in Horizontal Smooth and Micro-fin Tubes

Kookjeong Seo, Yongchan Kim*, Kyu-Jung Lee, Youn cheol Park

Department. of Mechanical Engineering, Korea University, Seoul, 136-701, Korea

Evaporation heat transfer coefficients and pressure drops were measured for smooth and micro-fin tubes with R-22 and R-410A. Heat transfer measurements were performed for 3.0 m long horizontal tubes with nominal outside diameters of 9.52 and 7.0 mm over an evaporating temperature range of -15 to 5°C, a mass flux range of 68 to 211 kg/m²s, and a heat flux range of 5 to 15 kW/m². It was observed that the heat transfer coefficient increased with mass flux. Evaporation heat transfer coefficients of R-22 and R-410A increased as the evaporating temperature dropped at a lower heat flux. Generally, R-410A showed the higher heat transfer coefficients than R-22 in the range of low mass flux, high heat flux and high evaporating temperature. Pressure drop increased with a decrease of evaporating temperature and a rise of mass flux. Pressure drop of R-22 was higher than that of R-410A at the same mass flux.

Key Words : Evaporation Heat Transfer Coefficient, Pressure Drop, Smooth Tube, Micro-Fin Tube, R-22, R-410A

Nomenclature

G	: Mass flux (kg/m ² s)
h	: Heat transfer coefficient (W/m ² K)
i_{fg}	: Latent heat of refrigerant (kJ/kg)
L	: Test section length (m)
L_x	: Length at each measurement point (m)
m	: Mass flowrate (kg/s)
p	: Pressure (N/m ²)
Q_{in}	: Average electric power input (W)
q	: Average heat flux (W/m ²)
T_e	: Evaporating temperature (K)
T_{in}	: Inlet temperature of refrigerant (K)
T_{out}	: Outlet temperature of refrigerant (K)
T_r	: Refrigerant temperature (K)
T_w	: Wall temperature (K)
$T_{w,in}$: Average inner wall temperature (K)
$T_{w,out}$: Average outer wall temperature (K)
x	: Vapor quality

1. Introduction

During the past decades, many aspects of boiling heat transfer have been investigated. However, the experimental data for alternative refrigerants of R-22, such as R-407C and R-410A, are limited in open literature. In addition, micro-fin tubes with smaller tube diameter have received increasing attention in recent years due to advantages in energy efficiency and compactness of a heat exchanger.

Schlager et al. (1990) reported the evaporation heat transfer coefficients for three micro-fin tubes with outside diameter of 12.7 mm having different fin height, number of fins and helix angle. The average evaporation heat transfer coefficients in the micro-fin tubes were 1.6 to 2.2 times larger than those in a smooth tube. Evaporating temperatures tested were 0 to 6°C, but the effect of heat flux was not discussed. Ha (2000) tested the performance of smooth and micro-fin tubes with an outside diameter of 9.52 mm using R-12. He reported that the heat transfer coefficient was a weak function of heat flux in the micro-fin tube.

* Corresponding Author,

E-mail : yongckim@korea.ac.kr

TEL : +82-2-3290-3366; FAX : +82-2-921-5439

Department. of Mechanical Engineering, Korea University, Seoul, 136-701, Korea. (Manuscript Received July 6, 2000; Revised May 17, 2001)

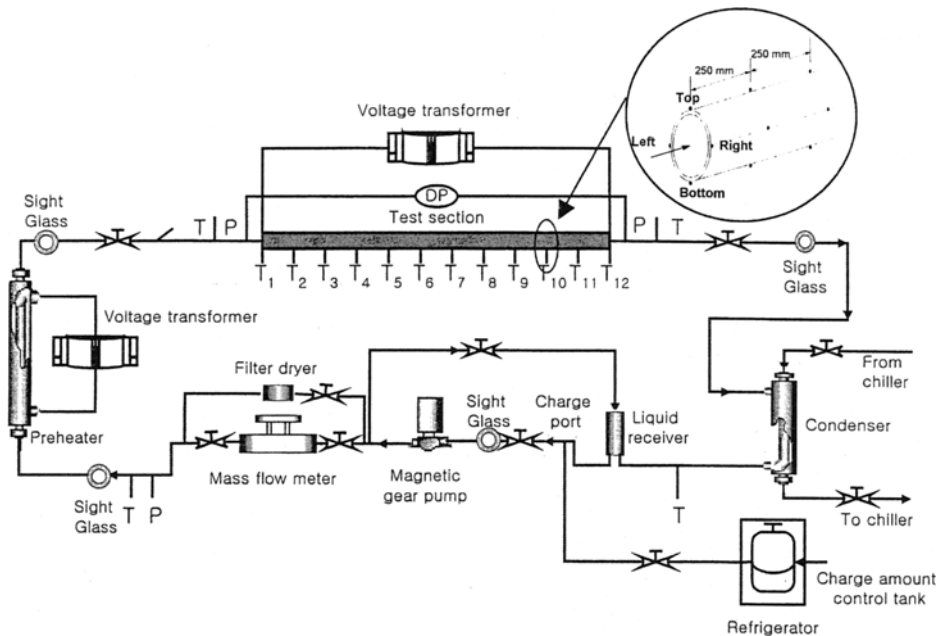


Fig. 1 Schematic of the experimental setup

Kuo and Wang (1995, 1996) tested the performance of micro-fin tubes with outside diameters of 9.52 and 7.0 mm using R-22. It was reported that the evaporation heat transfer coefficients increased with the mass flux, heat flux and evaporating temperature. The heat transfer enhancement factor (EF) for a 9.52 mm micro-fin tube was approximately equal to 2.2, while for a 7.0 mm micro-fin tube, EF was 1.6. The EF is defined as the ratio of the heat transfer coefficient of a micro-fin tube to that of a comparable smooth tube at similar test conditions.

When the heat pumps operate in a heating mode, evaporating temperatures range from -20 to 10°C , and are dependent on the outdoor temperature. Most of the previous studies on the evaporation heat transfer inside tubes were focused on evaporating temperatures above 0°C with high heat flux conditions. Furthermore, the effects of micro-fin tube and tube diameter on heat transfer characteristics were not generally reported in previous studies. Further study is required at lower evaporating temperatures with micro-fin tubes to enhance the performance of heat exchangers applied to heat pumps.

In the present study, the evaporation heat

transfer coefficients and pressure drops were measured for smooth and micro-fin tubes with R-22 and R-410A at low evaporating temperatures that were consistent with the operating conditions of heat pumps in the heating mode. The effects of heat flux, mass flux and inner diameter on the evaporation heat transfer and pressure drop were investigated. The test results for R-22 were also compared with those for R-410A as a function of operating parameters. In addition, the heat transfer enhancement of micro-fin tubes over smooth tube was evaluated.

2. Experimental Apparatus and Test Procedure

Figure 1 shows a schematic of the experimental setup. The test loop consists of a liquid pump, a preheater, a test section, and a condenser. The liquid pump with a variable speed motor was used to provide the specified mass flux passing through the test section. The inlet quality of the test section was adjusted by the electric power input supplied to the preheater. Superheated refrigerant at the exit of the test section was cooled using the condenser, and then returned to

Table 1 Dimension of the tubes tested

Parameter	Test tube		Micro-fin	
	Smooth	Micro-fin	Smooth	Micro-fin
Outside diameter(mm)	9.52	7.0	9.52	7.0
Average thickness(mm)	0.41	0.41	0.35	0.32
Average inside diameter(mm)	8.70	6.18	8.82	6.36
Maximum inside diameter(mm)	8.70	6.18	8.92	6.46
Fin-height(mm)	-	-	0.12	0.15
Helix angle $\beta(^{\circ})$	-	-	25	18
Number of fins	-	-	60	60
Inside surface Area(cm^2/m)	273.3	194.2	392.7	304.3
Surface Area Ratio($A_{\text{micro-fin}}/A_{\text{smooth}}$)	1.0	1.0	1.44	1.57

the liquid pump.

Since the liquid pump was utilized to circulate the refrigerant mass flow, the receiver located before the pump should have proper liquid level. When the saturation temperature is very low, liquid specific volume becomes lower and liquid level in the receiver decreases, which will result in unstable operation of the pump. Therefore, when the evaporating temperature varies very much, it is necessary to regulate the refrigerant charge amount into the system based on the saturation temperature. In the present experiments, an expansion tank was utilized to control the charge amount into the system. The refrigerant vessel that was kept inside of the refrigerator was connected to the suction side of the pump to allow easy regulation of refrigerant charge.

Table 1 shows the dimension of the test section. The tubes used in the present study were 3.0 m long with outer diameters (OD) of 9.52 and 7.0 mm. The average inner diameter (ID) of the smooth and micro-fin tube for the 9.52 mm OD was 8.70 and 8.82 mm, respectively, while for the 7.0 mm OD tube, it was 6.18 and 6.30 mm, respectively. The area used in the calculation of heat transfer coefficient and mass flux was based on the average inner diameter of the micro-fin tubes. The average inner diameter was calculated as the equivalent diameter having a wetted cross sectional area for the micro-fin tube.

The surface temperature of the test section was measured with thermocouples that were soldered

to the top, both sides, and bottom around the outer tube circumference at each location. The rope heater (2 mm OD) was wrapped around the thermocouple junctions. The test section was insulated with glass wool and double layers of rubber foam to reduce heat loss to the ambient. The heat loss to the surrounding was considered in determination of the heat flux using the calibration data.

The refrigerant flow rate was measured using a Coriolis effect flowmeter with uncertainty of $\pm 0.2\%$ reading. The pressure of the refrigerant entering the test section was monitored with a pressure transducer with uncertainty of ± 2.1 kPa, while the pressure drop across the test section was measured with a differential pressure transducer. All temperatures were measured using the T-type thermocouples with uncertainty of $\pm 0.1^{\circ}\text{C}$. The power inputs to the preheater and the test section were monitored using a power meter with uncertainty of $\pm 0.1\%$ of full scale.

Experiments were performed with R-22 and R-410A in the horizontal smooth and micro-fin tubes. Table 2 shows the range of experimental conditions. The refrigerant mass flux was varied from 70 to 211 $\text{kg}/\text{m}^2\text{s}$, and the evaporating temperature from -15 to 5°C at a heat flux of $5 \text{ kW}/\text{m}^2$. For a mass flux of $164 \text{ kg}/\text{m}^2\text{s}$, the heat flux was varied from 5 to $15 \text{ kW}/\text{m}^2$.

Table 2 Test conditions for smooth and micro-fin tubes

Heat flux: q (kW/m ²)		Evaporating temperature: T_e		
		-15°C	-5°C	5°C
Mass flux: G (kg/m ² s)	70	5kW/m ²	5kW/m ²	5kW/m ²
	117	5	5	5
	164	5	5	5
		10	10	10
	211	5	5	5

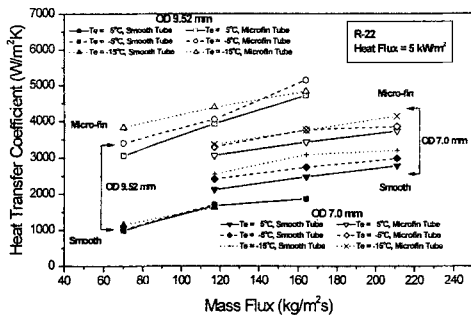


Fig. 2 Average heat transfer coefficients for R-22 as a function of mass flux

3. Data Reduction

The present experiments measure the flow boiling heat transfer coefficients of R-22 and R-410A. The definition of the local evaporation heat transfer coefficient is given by

$$h = \frac{q}{T_{w,in} - T_r} \quad (1)$$

where q represents the electric heating power per unit area, and $T_{w,in}$ and T_r are the inner wall temperature and refrigerant temperature, respectively, at a local point.

Since the internal horizontal two-phase flow is not symmetric due to gravitational effects, the inner wall temperature at a local point needs to be averaged over radial circumference. Due to difficulties in the measurement of inner wall temperature, the outer wall temperatures were measured using the thermocouples soldered to outer tube circumference (top, both sides, and bottom) as shown in Fig. 1. The average inner wall temperature $T_{w,in}$, is determined from $T_{w,out}$ employing

one-dimensional steady-state radial heat conduction equation through the tube wall. The average outer wall temperature is calculated by

$$T_{w,out} = \frac{T_{w,Top} + T_{w,Bottom} + T_{w,Left} + T_{w,Right}}{4} \quad (2)$$

Due to pressure drop during evaporation process, the refrigerant temperature decreases with an addition of tube length. The refrigerant temperature at a given length is determined by assuming linear profile along the tube length. The refrigerant temperature at a local point, T_r , is given by

$$T_r = T_{in} - (T_{in} - T_{out}) \times \frac{l_x}{l} \quad (3)$$

where T_{in} and T_{out} are the inlet and outlet refrigerant temperatures of the test section, respectively. The l_x is the tube length at a local point, and l is the length of the entire test section.

The local quality x at the test section is estimated by

$$\Delta x = \frac{Q_{in}}{m \cdot i_{fg}} \quad (4)$$

where m is mass flow rate, and Q_{in} is the power input to the test section.

The average heat transfer coefficient, \bar{h} , over the qualities tested is estimated by integrating the local heat transfer coefficient with respect to quality.

$$\bar{h} = \frac{\int_{x_{in}}^{x_{out}} h dx}{x_{out} - x_{in}} \quad (5)$$

Uncertainties of the heat transfer coefficients were estimated using a propagation of error analysis (Kline and McClintock, 1953). Uncertainties of the test parameters and heat transfer coefficients are given in Table 3. The physical and transport properties of refrigerants were evaluated using REFPROP 6.0.

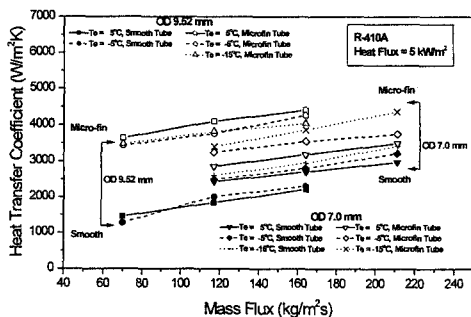
4. Experimental Results

4.1 Effects of mass flux, evaporating temperature, inner diameter and heat flux

Figure 2 shows the average heat transfer

Table 3 Uncertainties of operating parameters and heat transfer coefficients for R-22(R-410A)

parameter		Uncertainties					
$m(\text{kg/h})$		$\pm 0.2\%$ of reading					
$T(^{\circ}\text{C})$		$\pm 0.1^{\circ}\text{C}$					
$G(\text{kg/m}^2\text{s})$		$\pm 1.6\%$					
$q(\text{kW/m}^2)$		$\pm 1.8\%$					
Heat flux(kW/m^2)		$q=5$		$q=10$		$q=15$	
Outer diameter(mm)		9.52	7.0	9.52	7.0	9.52	7.0
$G=164$ ($\text{kg/m}^2\text{s}$)	Smooth	$\pm 5(6)\%$	$\pm 8(8)\%$	$\pm 3\%$	$\pm 4\%$	$\pm 3\%$	$\pm 3\%$
	Micro-fin	$\pm 19(12)\%$	$\pm 11(11)\%$	$\pm 6\%$	$\pm 5\%$	$\pm 4\%$	$\pm 4\%$

**Fig. 3** Average heat transfer coefficients for R-410A as a function of mass flux

coefficients of R-22 as a function of mass flux at a heat flux of 5 kW/m^2 . As expected, the heat transfer coefficient increased with mass flux, and it was strongly dependent on mass flux. These trends were also reported in most previous studies (Kuo and Wang, 1996; Schlager et al., 1990; Wijaya and Spatz, 1995). Generally, for the lower evaporating temperature and higher mass flux, the higher values of heat transfer coefficient were observed in the present experiments. Two-phase Reynolds number proposed by Chen (1966) is a function of liquid Reynolds number and Martinelli parameter. As the evaporating temperature decreases, two-phase Reynolds number increases with the same Martinelli parameter. Therefore, the higher heat transfer coefficient at the lower evaporating temperature might have resulted from a rise of the two-phase Reynolds number. The heat transfer coefficients for 9.52 mm micro-fin tube were the highest among the tubes tested. R-410A had the similar trends for the heat transfer coefficients as R-22, as shown in

Fig. 3.

Micro-fin tubes showed higher heat transfer coefficients than smooth tubes for all test conditions. For R-22, the heat transfer enhancement factor (EF) for 9.52 and 7.0 mm tubes varied from 2.3 to 3.3 and from 1.3 to 1.6, respectively. For R-410A, the EF for the 9.52 mm and 7.0 mm tubes ranged from 1.8 to 2.9, and from 1.1 to 1.5, respectively.

The effects of tube diameter on the heat transfer coefficient were drastically changed by varying tube surface from smooth to micro-fin shape. As shown in Figs. 2 and 3, the heat transfer coefficients for 7.0 mm smooth tube were approximately 39% and 25% higher than those for 9.52 mm smooth tube with R-22 and R-410A, respectively. However, the heat transfer coefficients for 9.52 mm micro-fin tube were approximately 31% and 22% higher than those for 7.0 mm micro-fin tube with R-22 and R-410A, respectively.

For an annular flow, convective transport of heat across a liquid film on the wall is strongly dependent on the vaporization liquid at the liquid-vapor interface of the film. It was reported that for evaporation with qualities from 0.2 to 0.8, the ratio of film thickness to fin height was less than unity (Kwak and Bai, 1999). As the ratio of film thickness to fin height decreased below unity, some portion of the micro-fin would be in a dryout state and the heat transfer enhancement rate obtained by micro-fin decreased. Therefore, an optimum film thickness to fin height is very important parameter to determine the heat

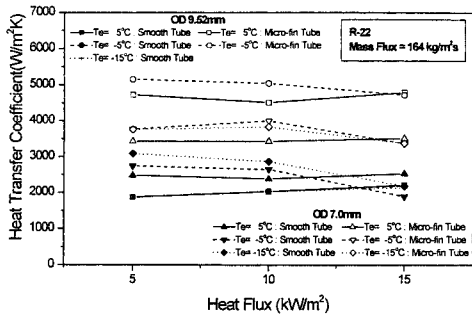


Fig. 4 Average heat transfer coefficients for R-22 as a function of heat flux

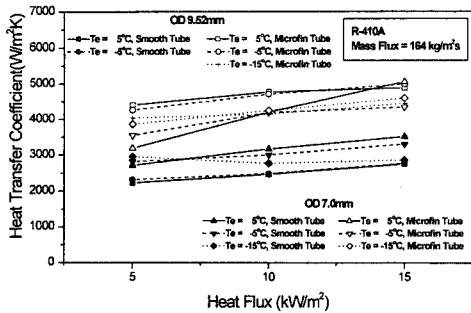


Fig. 5 Average heat transfer coefficients for R-410A as a function of heat flux

transfer enhancement during evaporation. Another important parameter would be a overflow probability that is the possibility of the flow between liquid films over a tip of micro-fin. Based on the test results, it can be hypothesized that the 9.52 mm OD micro-fin tube provides better film thickness conditions for the heat transfer enhancement over the comparable smooth tube than the 7.0 mm OD micro-fin tube does. The similar trend was presented in the data of Kuo and Wang (1995, 1996). However, Klimenko (1988) reported that the heat transfer coefficients were not strongly dependent on the tube diameter in a convective boiling region. Additional studies are necessary to verify the effects of tube diameter on the heat transfer coefficients for micro-fin tubes.

Figures 4 and 5 show the effect of heat flux on heat transfer coefficients for R-22 and R-410A, respectively, at a mass flux of 164 kg/m²s. The heat transfer coefficients for 7.0 mm tubes were affected more strongly with heat flux at a higher

evaporating temperature than those for 9.52 mm tubes. As shown in the Fig. 4, for lower evaporating temperatures, the heat transfer coefficients for R-22 dropped with an increase of heat flux. However, as shown in Fig. 5 the heat transfer coefficients for R-410A were proportional to heat flux for all evaporating temperatures tested. Generally, previous studies reported that the effect of heat flux on heat transfer coefficients was significant in the low quality region. Since an increase of heat flux promotes nucleate boiling at low qualities, the average heat transfer coefficient is enhanced. However, when the heat flux is relatively high for a given mass flux and evaporating pressure, a large portion of liquid film will be in a dryout state and the average heat transfer coefficient decreases. In addition, it was observed that the heat transfer coefficients at high evaporating temperatures were more sensitive to heat flux.

4.2 Comparison of R-410A with R-22

Figures 6 and 7 show the ratio of the heat transfer coefficient for 9.52 mm and 7.0 mm tubes, respectively, as a function of mass flux at a heat flux of 5 kW/m². For the smooth tubes, heat transfer coefficients for R-410A were of equal or higher values than those for R-22.

For 9.52mm OD micro-fin tube, as the mass flux increased, the ratio of heat transfer coefficient for R-410A to that for R-22 dropped relatively. Moreover, as the evaporating temperature decreased, the ratio reduced. Generally, R-410A has better thermophysical properties than R-22 in aspect of pool boiling heat transfer because of its lower surface tension, liquid viscosity and void fraction, higher specific liquid volume at a given saturation temperature. However, as mass flux increases and evaporating temperature decreases, nucleate boiling tends to be suppressed. Then, the changes of mass flux and evaporating temperature would provide beneficial effects for heat transfer performance of R-22. If these presumptions are adequate, the ratio between heat transfer coefficients of R-410A and R-22 relatively decreases with an increase of mass flux and a decrease of evaporating temperature. However, for

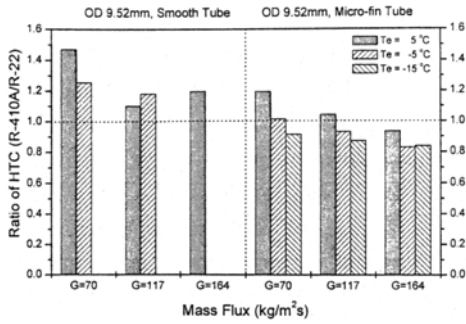


Fig. 6 Ratio of heat transfer coefficients with a heat flux of 5 kW/m² in 9.52 mm tube

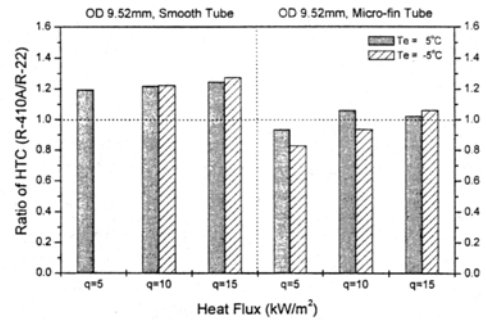


Fig. 8 Ratio of heat transfer coefficients with a mass flux of 164 kg/m²s in 9.52 mm tube

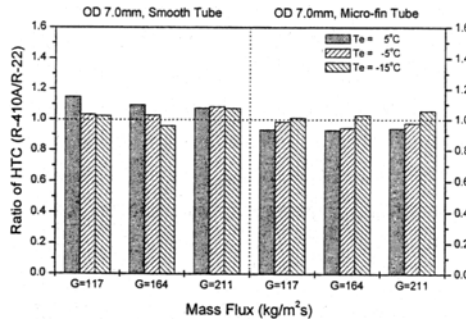


Fig. 7 Ratio of heat transfer coefficients with a heat flux of 5 kW/m² in 7.0 mm tube

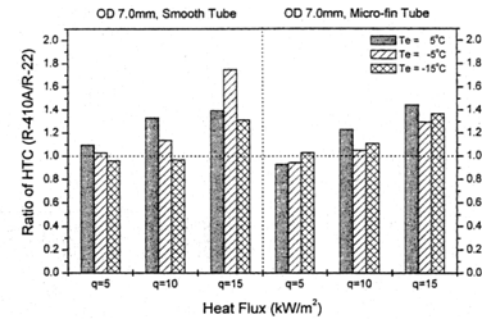


Fig. 9 Ratio of heat transfer coefficients with a mass flux of 164 kg/m²s in 7.0 mm tube

7.0 mm micro-fin tubes, the effects of mass flux on the ratio became less pronounced.

Figures 8 and 9 show the ratio of the heat transfer coefficient for 9.52 mm and 7.0 mm tubes, respectively, as a function of heat flux at a mass flux of 164 kg/m²s. For all tubes tested, the ratio increased with heat flux. Generally, the ratios for the smooth tubes were higher than those for the micro-fin tubes. In addition, heat transfer coefficients of R-410A were more sensitive to the heat flux than those of R-22.

4.3 Pressure drop

Figure 10 shows the pressure drop of R-22 per unit length for the smooth and micro-fin tubes. The pressure drop increased with mass flux due to an increase of flow velocity. In addition, the pressure drop increased significantly as the evaporating temperature decreased. An augmentation of liquid viscosity and specific volume of vaporized refrigerant with a reduction of

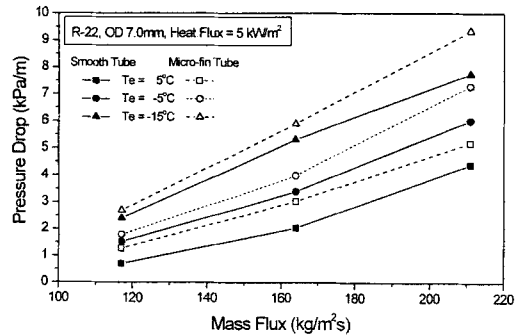


Fig. 10 Pressure drop as a function of mass flux for R-22

evaporating temperature leads to an increase of refrigerant velocity and pressure drop. The effect of mass flux on pressure drop in the micro-fin tubes was significantly higher than that in the smooth tube. The heat transfer coefficient and pressure drop increased with a reduction of evaporating temperature and rise of mass flux. As shown in Fig. 11, the trends of pressure drop

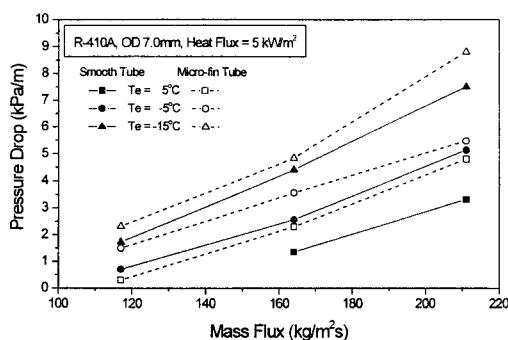


Fig. 11 Pressure drop as a function of mass flux for R-410A

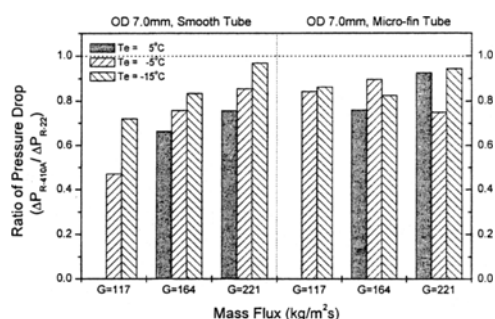


Fig. 12 Ratio of pressure-drop in 7.0 mm tube

for R-410A were similar to those for R-22. However, as shown in Fig. 12, the pressure drop for R-410A is smaller than that for R-22 due to lower values of viscosity and velocity.

The difference of the pressure drop between R-22 and R-410A was reduced with a decrease of evaporating temperature and increase of mass flux. The micro-fin tubes showed higher pressure-drop than the smooth tubes for all test conditions. Pressure drop penalty factors (PF) for the 7.0 mm tubes varied from 1.1 to 1.8 and from 1.1 to 2.1 for R-22 and R-410A, respectively.

5. Conclusions

In the present study, the evaporation heat transfer coefficients and pressure drops for R-22 and R-410A were measured and analyzed as a function of heat flux, mass flux, evaporating temperature, and tube diameter. The experiments were conducted for the smooth and micro-fin tubes with nominal outside diameters of 9.52 mm

and 7.0 mm.

For both refrigerants, the evaporation heat transfer coefficient was enhanced as the mass flux increased for the smooth and micro-fin tubes. The micro-fin inside a tube was more effective in the larger tube diameter in the range of present test conditions. For R-22, the EF for 9.52 and 7.0 mm tubes varied from 2.3 to 3.3 and from 1.3 to 1.6, respectively. For R-410A, the EF for 9.52 and 7.0 mm tubes ranged from 1.8 to 2.9, and from 1.1 to 1.5, respectively. The heat transfer coefficients of R-410A were higher than those of R-22 in the range of lower mass fluxes, higher heat fluxes and higher evaporating temperatures.

The pressure drop increased with a decrease of evaporating temperature and increase of mass flux. The pressure drop for R-410A was smaller than that for R-22 due to lower viscosity and velocity. As the evaporating temperature decreased and the mass flux increased, the difference of pressure drop between R-22 and R-410A was reduced.

Acknowledgements

This work was supported by Korea Research Foundation Grant (KRF-97-005-E00198).

References

- Chen, J. C., 1966, "Correlation for Boiling Heat Transfer to Saturated Fluids in Convective Flow," *I&EC Process Design and Development*, Vol. 5, No. 3, pp. 322~329.
- Ha, S. C., 2000, "Some Aspects of Experimental In-Tube Evaporation," *KSME International Journal*, Vol. 14, NO. 5, pp. 537~546.
- Klimenko, V. V., 1988, "A Generalized Correlation for Two-phase Forced Flow Heat Transfer," *International Journal of Heat and Mass Transfer*, Vol. 31, No. 3, pp. 541~552.
- Kline, S. J. and McClintock, F. A., 1953, "Describing Uncertainties Single Sample Experiments," *Mechanical Engineering*, Vol. 75, pp. 3~8.
- Kuo, C. S. and Wang, C. C., 1996, "In-tube Evaporation of HCFC-22 in a 9.52 mm Micro-

fin/Smooth Tube," *International Journal of Heat and Mass Transfer*, Vol. 39, No. 12, pp. 2559 ~2569.

Kuo, C. S., Wang, C. C., Cheng, W. Y. and Lu, D. C., 1995, "Evaporation of R-22 in a 7 mm Micro-fin Tube," *ASHRAE Transactions*, Vol. 95, pp. 1055~1061.

Kwak, K. M. and Bai, C. H., "A Discussion to the Heat Transfer of Microfin Tube by Fin Geometry," *Proceeding of SAREK Summer Meeting*, pp. 897~902.

Schlager, L. M., Pate, M. B. and Bergles, A. E., 1990, "Evaporation and Condensation Heat

Transfer and Pressure Drop in Horizontal, 12. 7-mm Micro-fin Tubes with Refrigerant 22," *Transactions of the ASME, Journal of Heat Transfer*, Vol. 112, Nov., pp. 1041~1047.

Wang, C. C., Kuo, C. S., Chang, Y. J. and Lu, D. C., 1996, "Two-Phase Flow Heat Transfer and Friction Characteristics of R-22 and R-407c," *ASHRAE Transactions*, Vol. 96, pp. 830~838.

Wijaya, H. and Spatz, M. W., 1995, "Two-Phase Flow Heat Transfer and Pressure Drop Characteristics of R-22 and R-32/125," *ASHRAE Transactions*, Vol. 101, pp. 1020 ~1027.